



Manuscript id: ZUMJ-2411-3692

Doi: 10.21608/ZUMJ.2024.337569.3692

**ORIGINAL ARTICLE**

## **PARG Inhibition Modulates Viability, Clonogenicity, and Migration of Breast Cancer Cells. Response to Radiotherapy**

Shaymaa E. El Feky <sup>1\*</sup>, Nermin A. Bekheet <sup>2</sup>, Fawziya A.R. Ibrahim <sup>3</sup>, Nadia A. Abd El Moneim <sup>4</sup>, Mohammed Salama <sup>5</sup>, Marwa M Essawy <sup>6,7</sup>, Medhat Haroun <sup>2</sup>

<sup>1</sup> Radiation Sciences Department, Medical Research Institute, University of Alexandria, Alexandria, Egypt.

<sup>2</sup> Department of Biotechnology, Institute of Graduate Studies and Research, University of Alexandria, Alexandria, Egypt.

<sup>3</sup> Applied Medical Chemistry Department, Medical Research Institute, University of Alexandria, Alexandria, Egypt.

<sup>4</sup> Cancer Management and Research Department, Medical Research Institute, University of Alexandria, Alexandria, Egypt.

<sup>5</sup> Histochemistry and Cell Biology and Department, Medical Research Institute, University of Alexandria, Alexandria, Egypt.

<sup>6</sup> Oral Pathology Department, Faculty of Dentistry, University of Alexandria, Alexandria, Egypt.

<sup>7</sup> Center of Excellence for Research in Regenerative Medicine and Applications (CERRMA), Faculty of Medicine, University of Alexandria, Alexandria, Egypt.

### **Corresponding author**

Shaymaa Essam El Feky

Email:

[shaymaa.elfeky@alexu.edu.eg](mailto:shaymaa.elfeky@alexu.edu.eg)

**Submit Date: 25-11-2024**

**Accepted Date: 01-12-2024**

### **ABSTRACT**

**Background:** Targeting DNA repair through inhibition of poly (ADP-ribose) glycohydrolase (PARG) enzyme is a promising strategy to modulate cancer resistance to traditional therapy. In the present work, we evaluated the possible modifying effect of PARG inhibition in breast cancer cell lines' response to DNA damage induced by radiotherapy.

**Methods:** Breast cancer cell lines (MCF-7 and MDA-MB-231) were exposed to different doses of ionizing radiation (IR) either with or without PDD00017273, a PARG inhibitor, and evaluated cellular response after 48 hours. MTT assay was utilized to evaluate cellular viability, clonogenic assay, and migration assay were performed, relative gene expression of PARG and apoptosis-inducing factor (AIF) was evaluated using real-time PCR, and protein expression of PARG was detected using immunostaining.

**Results:** Our findings showed that PARGi prior to irradiation treatment significantly increased PARG expression on both gene and protein levels, which was accompanied by a significant drop in cellular viability in both cell lines compared to IR alone. These results were further confirmed by the upregulated expression of the AIF gene. Cellular clonogenicity and migration have declined significantly in cells treated with PARGi + IR combination rather than IR alone.

**Conclusions:** Our study highlights the effect of PARGi in radio-sensitizing breast cancer cell lines, emphasizing its role in undermining the mechanisms of repairing DNA and increasing its sensitivity to IR.

**Keywords:** PARG; DNA repair; Breast Cancer; Radiotherapy; Radiosensitizer.

### **INTRODUCTION**

**B**reast cancer (BC) ranked second globally in respect of incidence, and it contributes

significantly to women's mortality worldwide [1]. Amongst the different molecular subtypes of BC, Triple-negative breast cancer is the most aggressive

BC subtype, representing approximately 10-20% of all breast cancers, and designated by its poor outcome with higher metastatic potentials compared to the other subtypes [2]. Many traditional cancer treatments target tumor cells by inducing DNA damage either directly or indirectly causing cellular death. Agents like ionizing radiation (IR) result in single and double-strand breaks, mismatches, strand crosslinks, chemical alteration of nitrogenous bases or sugar backbone, or other DNA lesions [3, 4]. Nevertheless, several tumors develop a network of complex defense mechanisms targeting DNA lesions, including the overactivation of DNA repair pathways [5]. Therefore, targeting DNA repair pathways can sensitize tumors to DNA damage-based therapeutics [6].

Amongst the promising approaches in cancer treatment, the action of targeting poly(ADP ribosyl) has attracted considerable attention over the past few years. The PARylation process starts with Poly (ADP-ribose) polymerase (PARP) binding to DNA lesions – either single or double- after receiving a signal of DNA damage [7]. The PARylation of chromosomal proteins and poly (ADP-ribose) (PAR) moieties formation act as a sign for calling repair factors to the damaged site. Then, for DNA to be fixed, PAR should be degraded by the enzyme poly (ADP-ribose) glycohydrolase (PARG), which is a protein that reverses the action of PARP [8]. This dePARylation mediated by PARG functions as a crucial downstream phase of the PARylation process rather than an opposing step. In particular, PARG is essential for proper cellular repair mechanisms, DNA single- and double-strand breaks' repair, and the release of repair factors from PARylation clusters at the DNA-damaged locations [9].

The PARylation process was targeted by many PARP inhibitors, including olaparib, niraparib, rucaparib, and other drugs, which target DNA repair and cause cell death by interfering with DNA repair in cancer cells [10]. However, resistance against PARP inhibitors (PARPi) has recently emerged. Mechanisms of developing PARPi resistance include homologous repair restoration, BRCA gene reversion mutations, replication fork stabilization, and loss of PARP trapping [11]. For this reason, shifting to PARG inhibitors (PARGi) was one of the possible options that have shown promising effects in cancer therapy [12]. It was reported that PARG inhibition prolongs PARylation at DNA-damaged sites, traps DNA damage response proteins, and suppresses cancers that are resistant to PARPis [13].

Thus, a plethora of PARGis have emerged in recent years, and they were reported to exhibit encouraging potential as cancer therapies either alone or when administered concurrently with other cytotoxic agents [14].

We herein intended to weigh the possible modifying effect of PARG inhibition using PDD00017273 in the response of BC cell lines to DNA damage induced by radiotherapy.

## METHODS

### *Cell culture:*

MCF-7 (invasive ductal carcinoma) and MDA-MB-231 (triple negative adenocarcinoma) (ATCC, Virginia, US) were grown in Dulbecco's modified Eagle's medium (DMEM) with 10% (w/v) fetal bovine serum (FBS), penicillin (100 U/ml) and streptomycin (100 U/ml) (Gibco, US). The cells were incubated in 5% CO<sub>2</sub> air at 37 °C until 75-80% confluent monolayer.

### *Treatment of cell lines:*

Plates containing MCF-7 and MDA-231 cells (96, 12 and 6-well plates according to subsequent assay) were treated with 0.3 μM PDD00017273 (PARGi) (Sigma Aldrich, US), that was either combined X-rays at 2, 4, 6, 8 and 10 Gy doses delivered by Linear Accelerator (PRIMUSTM, Siemens® Medical Solutions, Inc.). the field of IR exposure was set to 20x25 cm dimensions, plates were positioned in the dose isocenter the distance between the isocenter and IR source was 97 cm, the dose rate was set to 300 MU/min and a phantom was used to verify the IR dose homogeneity. All treatment combinations were done in triplicates.

### *MTT Assay:*

The modifying effect of PARGi on cellular response to IR was evaluated using the colorimetric MTT (3-(4, 5-dimethylthiazol-2-yl)-2, 5-diphenyltetrazolium bromide) (SERVA-Electrophoresis GmbH, Germany) assay was utilized to assess cellular viability 48 h after treatment. Culture plates (96 wells) were seeded with 7000 cells and incubated for 24 h. Forty-eight hours post-treatment, viability was assessed by adding 100 μL of 5 mg/ml MTT according to the previously reported method [15]. After four hours, the media was discarded, and the resultant formazan crystals were dissolved using 100 μL Dimethyl sulfoxide (DMSO, Fisher Chemical, UK). The intensity of the formed color was read by a spectrophotometer (Infinite F15 TECAN, Switzerland) at 570 nm. The % of viable cells was estimated by the equation: Viable cell % = (OD treated/OD untreated) × 100, where "OD" is

the optical density. The % of cell viability was utilized to define the lethal dose (LD50) values of each treatment. The effectiveness of PARGi in modifying cellular response to IR was assessed by calculating the dose modification factor (DMF) using the equations:  $DMF_{rad} = (LD50 \text{ of PARGi} + IR) / (\text{Radiation LD50 of IR})$ .

#### **Cell Migration Assay:**

Confluent monolayers of MCF-7 and MDA-MB-231 cells were obtained by seeding  $3 \times 10^5$  cells in each well of 6-well plates. To make a straight line that is free of cells, a cut was made using a pipette tip before applying the planned treatments. The scratches were photographed at the beginning and after 48 h of treatment by an inverted microscope (Olympus, Japan, x100 magnification) [16]. We analyzed the scratch area images by ImageJ software and calculated the area of the wound and the % of wound closure.

#### **Colony-Forming Assay:**

The assay was performed by seeding culture plates (6 wells) with 500 cells/well, allowing growth at the previously mentioned conditions for six hours and allowing cells to adhere. Cells were treated as formerly described for 48 h, then the medium was replaced with a drug-free medium and followed up for 10 to 14 days until colonies were formed. To fix the formed colonies, phosphate-buffered saline (PBS) was used to wash the colonies, and Crystal Violet (Sigma-Aldrich, Burlington, MA, USA) was used to stain the colonies at a concentration of 3% (w/v). Plates were photographed, and images were analyzed using ImageJ software to determine the number of colonies in each group [17].

#### **Evaluation of gene expression by Quantitative Real-time PCR:**

Quantitative real time PCR (qRT-PCR) was used for the quantitative determination of the relative expression of PARG and apoptosis inducing factor (AIF). Isolation of RNA in treated cells was done using Qiagen RNeasy Mini Kit (Hilden, Germany, cat#74104) according to the manufacturer's instructions. RNA concentration in samples and quality of purification were determined using an ND2000 Nanodrop Spectrophotometer (Thermo Fisher Scientific Co, Waltham, Massachusetts, USA). To prepare complementary DNA (cDNA) samples, 20 ng/ $\mu$ L RNA samples were reverse transcribed using the high-capacity cDNA reverse transcription kit (Life Technologies #4374966). The thermal cycler conditions were 25 °C for 10 min, 37 °C for 120 min, 85 °C for 5 s, and four °C on hold.

For qRT-PCR, 1  $\mu$ l of cDNA was mixed with 12.5  $\mu$ l Maxima SYBR Green master mix (Thermo Fisher Scientific Co, Waltham, Massachusetts, USA), 1  $\mu$ l of 0.3  $\mu$ M forward and reverse primers each, 0.5  $\mu$ l ROX buffer, and 9  $\mu$ l nuclease-free water. The primers' sequences were: PARG forward: 3' AGTGGCTTGGAACTCCCATTGAG 5', reverse: 3' ACTTCTCCTGCTCGCAAAAGATC 5', AIF: 3' GGCTTCCTTGGTAGCGAACTGG 5', reverse: 3' GTCCAGTTGCTGAGGTATTCGG 5', GAPDH forward, 5'- TCAAGATCATCAGCAATGCC-3' and reverse, 5'- CGATACCAAAGTTGTCATGGA-3'. The reaction conditions were: pre-treatment at 2 min at 50 °C, initial denaturation of 10 min at 95 °C, repeated 45 cycles of 15 sec at 95 °C (denaturation), 30 sec at 55 °C (annealing) and 30 sec at 72 °C (extension). The expression of the PARG and AIF genes was normalized to the reference gene GAPDH, and the  $2^{-\Delta\Delta Ct}$  method was used to calculate the fold change.

#### **Determination of PARG protein expression by immunocytochemistry (ICC):**

MCF-7 and MDA-MB-231 cells were grown on coverslips coated with poly-L-lysine and fixed in 6 well plates after sterilization using UV light for four h until 75% confluent monolayer was obtained, then cells were treated as mentioned above. Forty-eight hours post-treatment, PBS containing 0.1% Tween 20 was used to wash the cells after media removal. Fixation was then done using 4% paraformaldehyde in 7.4 pH at room temperature for 10 min. For permeabilization, incubation of coverslips for 10 min in PBS with 0.1% Triton X. The coverslips were immersed in heated antigen retrieval buffer (100 mM Tris, 5% [w/v] urea, pH 9.5, 95 °C) for 10 min and washed. For blocking, cells were incubated cells with 1% BSA, 22.52 mg/mL glycine in PBST (PBS+ 0.1% Tween 20) for 30 min. PARG monoclonal antibody (Cell Signaling Technology, USA) prepared in PBST with 1% BSA was incubated with cells at a concentration of 1:100 overnight at four °C in a humidified chamber. Before the incubation with the secondary antibody, the cells were washed 3 times in PBS for 5 min each. A secondary antibody was prepared in 1% BSA, and incubation was done for one hour at room temperature. To visualize the reaction, a streptavidin-biotin immunoperoxidase detection kit and 3-amino-9-ethylcarbazole (AEC) chromogen (Labvision, USA) based on the manufacturer's instructions with necessary modifications. Finally, cells were counterstained with Meyer's

hematoxyline (DakoCytomation, Denmark), mounted, and studied under the light microscope [18].

### STATISTICAL ANALYSIS

Statistical analysis of the obtained data was done using IBM SPSS software package version 20.0. (Armonk, NY: IBM Corp). Mean and standard deviation were used to describe quantitative data, and the level of statistical significance was judged at the 5% level. ANOVA test was used to compare between more than two groups of normally distributed quantitative variables, and pairwise comparisons were done using the Post Hoc test (Tukey) test. Student t-test For normally distributed quantitative variables.

### RESULTS

#### ***PARGi Decreased the Cellular Viability of MCF-7 and MDA-MB-231 cells and Induces Apoptosis When Combined with Ionizing Radiation:***

The results in Figure (1a) indicate the percentage of viable MCF-7 and MDA-MB-231 cells using MTT assay 48 hr post-treatment, taking the untreated cells as a control. A dose-dependent decrease in cellular viability was observed upon exposure to ionizing radiation with a lethal dose (LD50) of 7.5 and 14.5 for MCF-7 and MDA-MB-231, respectively ( $p < 0.05$ ). When cells were treated with 0.3  $\mu\text{M}$  PARGi prior to irradiation, the viability decreased significantly with LD50 of 5.4 and 7.7 for MCF-7 and MDA-MB-231 respectively ( $p < 0.05$ ). Therefore, PARGi has successfully decreased the LD50 by a DMF of 1.4 for MCF-7 and 1.9 for MDA-MB-231.

The results of MTT were further confirmed by quantitative determination of the relative expression of AIF. Our results indicate that AIF was significantly upregulated in MCF-7 and MDA-MB-231 cells exposed to 4, 6, and 8 grays as compared to the untreated control cells ( $p < 0.05$ ), peaking at 8 Gy. Treatment of cells with 0.3  $\mu\text{M}$  PARGi combined with different radiation doses significantly upregulated the gene expression of AIF as compared to cells treated with radiation doses alone ( $p < 0.05$ ) (Fig. 1b).

#### ***PARGi Downregulated the Expression of PARG when Combined with Ionizing Radiation Gene and Protein Levels:***

We examined the expression of PARG both on gene and protein levels, as presented in Figure

(2a). For both MCF-7 and MDA-MB-231 cells treated with IR, the relative expression of PARG was significantly higher than untreated cells, peaking at 4 Gy and then declining in a dose-dependent manner ( $p < 0.001$ ). The combination of IR with PARGi led to a significant decrease in PARG expression ( $p < 0.001$ ) to a level that it was no longer significantly higher than the control at 10 Gy. These patterns of expression were also confirmed by ICC detection of PARG protein in both cell lines, where the treatment with either IR has evoked the cellular expression of PARG protein as compared to untreated control cells and cells treated with PARGi alone. However, upon a combination of PARGi with either IR, the level of PARG protein was drastically downregulated (Fig. 2b).

#### ***PARGi suppresses the migration ability of cells when combined with Ionizing Radiation:***

The results of wound closure for all treatment combinations 48 h post-treatment relative to wound width for control untreated cells at 0 h are presented in Figure (3). Regarding the radio-modifying effect of PARGi on cell migration, a significant decrease in wound closure was observed in MCF-7 cells compared to cells exposed to IR alone. The percentages of wound closure were 66.05% and 46.15% for cells treated with 0.3  $\mu\text{M}$  PARGi prior to exposure to 4 Gy and 8 Gy I, R, respectively. These were significantly lower than respective groups treated with the same doses of IR alone (82.73% and 66.81% for 4 Gy and 8 Gy, respectively) ( $p < 0.05$ ). Nevertheless, the effect of PARG inhibition on MDA-MB231cells migration was minimal compared to MCF-7 as it was only significant for cells exposed to 8 Gy IR as the wound closure was 66% compared to 100% in cells exposed to IR alone ( $p < 0.05$ ).

#### ***PARGi Impedes the Clonogenic Ability of Cells when Combined with Ionizing Radiation:***

Our results revealed a significant sensitizing effect of PARG inhibition for IR represented in decreasing the clonogenic ability of both MCF-7 and MDA-MB-231 cells compared to the control group (Fig. 4). While the exposure to 8 Gy IR led to a reduction in the number of colonies to 53.3% and 62.2% for MCF-7 and MDA-MB-231 respectively. A further reduction in clonogenic ability to 19.0% and 8.9% for respective cell lines was observed in PARGi-IR combination groups ( $p < 0.05$ ).

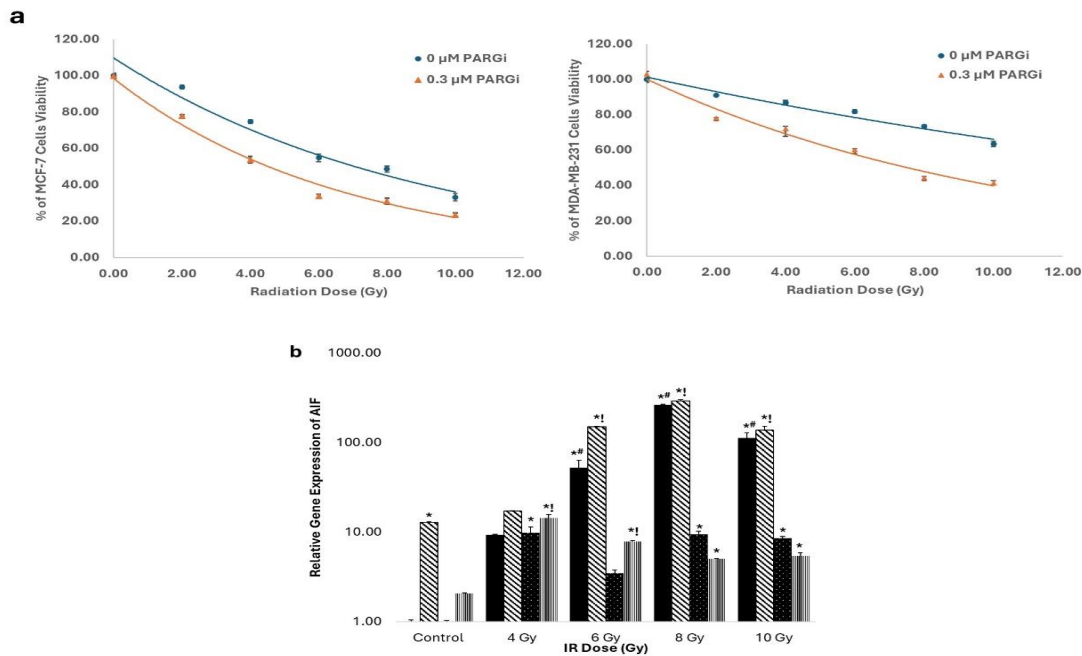


**Figure 1:** Viability Assays: a) MTT result of cell viability of control, 0.3  $\mu$ M PARGi-treated MDA-MB-231 and MCF-7 cells either alone or in combination with IR (0, 2, 4, 6, 8, and 10 Gy), b) Graphs of relative gene expression of AIF in MCF-7 and MDA-MB-231 48 h after being treated with IR (0, 4, 6, 8, or 10 Gy) with/without 0.3  $\mu$ M PARGi, where \* represent significant difference from control group, # significant difference from lower IR dose treated groups,! Represent significant difference from respective PARGi untreated groups, n=3, p<0.05.

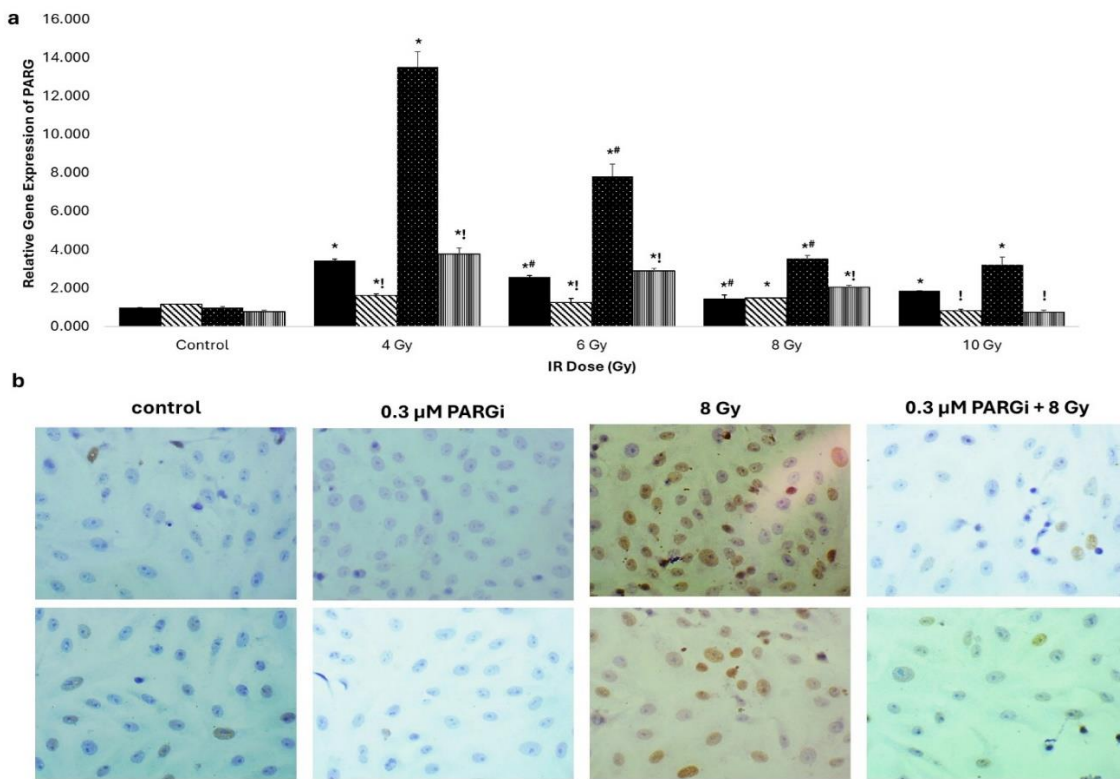


**Figure 2:** a) Graphs of relative gene expression of PARG in MCF-7 and MDA-MB-231 48 h after being treated with IR (0, 4, 6, 8, or 10 Gy) with/without 0.3  $\mu$ M PARGi, where \* represents a significant difference from the control group, # significant difference from lower IR dose treated groups,! Represent significant difference from

respective PARGi untreated groups, n=3, p<0.05. b) Immunostaining of MCF7 cells with PARG antibody for control and 48 h following treatment with 8 Gy IR, 0.3 μM PARGi, and their combination at 400x magnification.

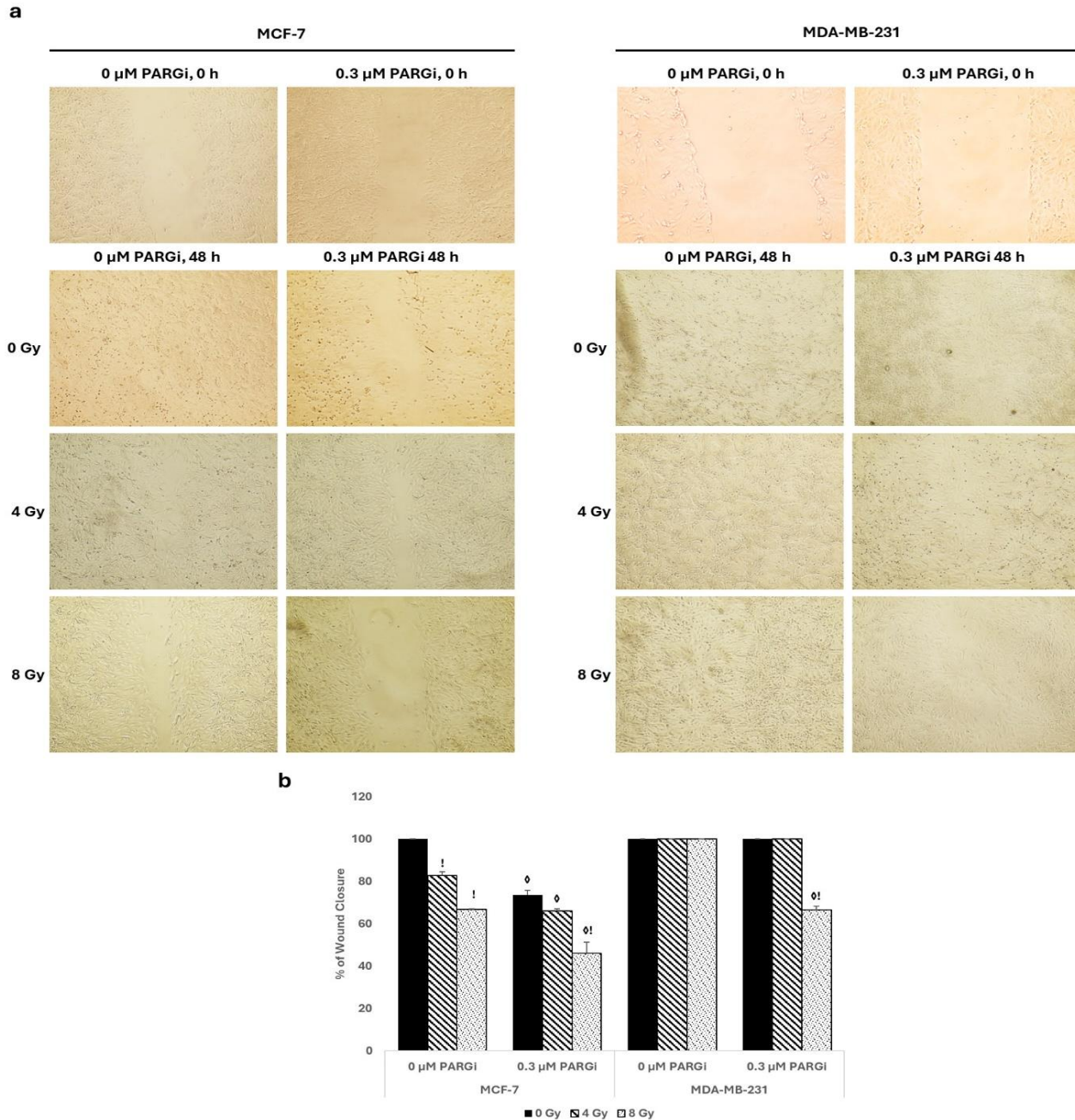


**Figure 3:** Migration Assay a) Pictures of MCF-7 and MDA-MB-231 cells wound healing assay for control at 0 h and cells treated with 0, 4, and 8 Gy IR with and without 0.3 μM PARGi 48 h after treatment. b) graphical presentation of % of wound closure compared to the control group at 0 h, where, ! Represent significant difference from respective IR untreated groups, ◊ represent a significant difference from respective PARGi untreated groups, n=3, p<0.05.

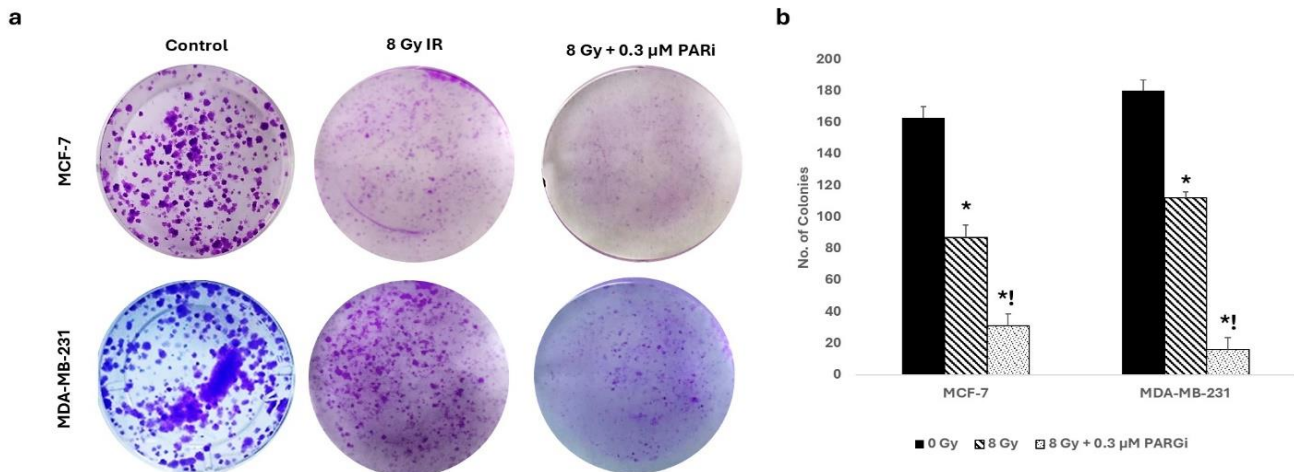


**Figure 4:** Clonogenic Assay a) Pictures of MCF-7 and MDA-MB-231 colonies 48 h after being untreated or treated with 8 Gy IR with/without 0.3 μM PARGi. b) Figure also shows a graphical presentation of the number of colonies in each group, where \* represents a significant difference from respective IR untreated groups! Represent significant difference from respective PARGi untreated groups, n=3, p<0.05.

### DISCUSSION

The response of tumors to the damaging effects of radiotherapy is a major contributing factor in determining their therapeutic outcomes [19]. Therefore, exploring agents that may reverse the mechanisms underlying resistance might be a propitious approach for the evolution of more effective treatment plans. In the current study, we showed that PARGi significantly modified cellular response to IR, which represented decreased cell viability and induced apoptosis. As IR is known to induce cellular death by causing single and double-strand breaks that weaken DNA's integrity, interference with the DNA repair through PARG inhibition decreases cellular resistance and renders the cells more sensitive to traditional therapeutic agents by a significant factor. These results are consistent with previous studies reported that after PARG silencing, sensitized hepatocellular carcinoma [20] and ovarian cancer [21] cell lines to strand breaks induced by X-Ray.

The decrease in cellular viability in response to PARG inhibition was accompanied by a significant downregulation of PARG gene expression in response to combining IR with PARGi. As IR induces cellular stress and DNA breaks, which activates the PARP enzyme to initiate the repairing pathway, and in turn PARG enzyme is over-expressed [22], compared to control, to facilitate PARP enzyme function as the PARylation cycle's opposing arms, synthesis and degradation, are represented by PARP and PARG [23], and upon

using PARGi PDD00017273, PARG enzymatic activity was blocked and its expression was down-regulated compared to cells treated with IR alone [24, 25]. Furthermore, many studies have reported the initial upregulation of PARG mRNA and protein in malignant cancers compared to its expression in normal cells [26, 27], which implicates its vital role in cancer cell survival and that its downregulation might have a vital role in repair process disruption and hence induction of cancer cell death.

Our results also indicate that the reduction in cellular viability and apoptosis induction is mediated by AIF, which was significantly higher in cells treated with PARGi prior to radiation. Our findings here are consistent with Cohausz et al., who reported that PARG inhibition could lead to the augmented signal of AIF gene expression while using ADP (hydroxymethyl) pyrrolidine-diol as a PARG inhibitor on mouse embryonic fibroblasts and human cervical carcinoma cells [28]. PARGi augments PAR accumulation which increases the dsDNA breaks in cells treated with IR [29]. Marked accumulation of PAR leads to decreased NAD<sup>+</sup> levels and increased ATP consumption to resynthesize NAD<sup>+</sup>, which results in impaired mitochondrial permeability, the release of AIF and cytochrome c, and activated caspase-independent cell death or, in other words, AIF-mediated PAR-dependent cell death [30].

We also showed that PARG targeting enhanced the effects of radiotherapy on the reduction of BC cell lines' clonogenic ability. This

reduction in cellular proliferation is consistent with the reduction in cellular viability, thus decreasing the number of colonies following treatment. A previous study indicated that MDA-MB-231 BC cells showed the largest response in the clonogenic survival assay compared with different cell lines [28]. Previous research also showed that the combination effect of PARGi and cytotoxic agents affected the proliferative abilities of different types of cancer cell lines. It was reported that PARG knockdown also decreased clonogenic activity in hepatocellular carcinoma exposed to X-rays [31]. PARGi also slowed down cellular migration, reaching its maximum level after 48 hours, depending on the cell line type.

To conclude, our study highlights the role of PARGi in sensitizing BC cell lines to IR, which emphasizes its role in undermining DNA repair mechanisms and increasing their sensitivity to DNA-damaging agents. The combination of PARGi with IR decreased cellular viability, increased apoptotic response, decreased clonogenicity, and cellular migration compared to cells treated with IR alone. Further studies on the mechanisms underlying this response in other BC cell lines, especially those with PARPi resistance, are recommended. Our results support the development of directions to include PARGi-radiotherapy combinations for better response in cancers that develop resistance to IR.

#### **Disclosure of potential conflicts of interest**

None

#### **Funding information**

None

#### **Contributors**

Conceptualization, S.E.E., F.A.R.I., N.A.A. and M.H.; Methodology, S.E.E., N.A.B., F.A.R.I., and M.S. Cell Culture Assays: S.E.E., N.A.B. & M.M.E.; Molecular Investigations, S.E.E., N.A.B. & F.A.R.I.; Immunostaining and examination: M.S. Data analysis and interpretation, S.E.E., N.A.B., F.A.R.I., & N.A.A.; Figures and graphical presentations: S.E.E., Draft preparation, S.E.E. and F.A.R.; All authors revised the manuscript.

#### **Ethical Approval**

The study was approved by the Ethical Committee of the Institute of Graduate Studies and Research (IGSR), University of Alexandria, on 9/2020.

#### **REFERENCES**

1. Bray F, Laversanne M, Sung H, Ferlay J, Siegel RL, Soerjomataram I, et al (2024) Global cancer statistics 2022: GLOBOCAN estimates of incidence and mortality worldwide for 36 cancers in 185 countries. *CA Cancer J Clin* 74:229-63. doi: 10.3322/caac.21834
2. Ensenyat-Mendez M, Llinàs-Arias P, Orozco JIJ, Íñiguez-Muñoz S, Salomon MP, Sesé B, et al (2021) Current Triple-Negative Breast Cancer Subtypes: Dissecting the Most Aggressive Form of Breast Cancer. *Front Oncol* 11:681476. doi: 10.3389/fonc.2021.681476.
3. Waks AG, Winer EP (2019) Breast Cancer Treatment: A Review. *JAMA* 321(3):288-300. doi: 10.1001/jama.2018.19323. PMID: 30667505.
4. Chatterjee N, Walker GC (2017) Mechanisms of DNA damage, repair, and mutagenesis. *Environ Mol Mutagen* 58(5):235-63. doi: 10.1002/em.22087.
5. Li L-y, Guan Y-d, Chen X-s, Yang J-m, Cheng Y (2021) DNA Repair Pathways in Cancer Therapy and Resistance. *Front Pharmacol* 11:629266. doi: 10.3389/fphar.2020.629266
6. Trenner A, Sartori AA (2019) Harnessing DNA Double-Strand Break Repair for Cancer Treatment. *Front Oncol* 9:1388. doi: 10.3389/fonc.2019.01388.
7. Jeong KY, Park M (2021) Poly adenosine diphosphate-ribosylation, a promising target for colorectal cancer treatment. *World J Gastrointest Oncol* 13(6):574-88. doi: 10.4251/wjgo.v13.i6.574.
8. Slade D (2020) PARP and PARG inhibitors in cancer treatment. *Genes Dev* 34(5-6):360-94. doi: 10.1101/gad.334516.119.
9. Kassab MA, Yu LL, Yu X (2020) Targeting dePARylation for cancer therapy. *Cell Biosci* 10:7. doi:10.1186/s13578-020-0375-y.
10. Turk AA, Wisinski KB. PARP inhibitors in breast cancer: Bringing synthetic lethality to the bedside (2018) *Cancer* 124(12):2498-506. doi: 10.1002/cncr.31307.
11. Giudice E, Gentile M, Salutari V, Ricci C, Musacchio L, Carbone MV, et al (2022) PARP Inhibitors Resistance: Mechanisms and Perspectives. *Cancers (Basel)* 14(6):1420. doi: 10.3390/cancers14061420.
12. Martincuks A, Zhang C, Austria T, Li YJ, Huang R, Lugo Santiago N, et al (2024) Targeting PARG induces tumor cell growth inhibition and antitumor immune response by reducing phosphorylated STAT3 in ovarian cancer. *J Immunother Cancer* 12(4):e007716. doi: 10.1136/jitc-2023-007716. PMID: 38580335; PMCID: PMC11002370.
13. Gogola E, Duarte AA, de Ruiter JR, Wiegant WW, Schmid JA, de Bruijn R, et al (2018) Selective Loss of PARG Restores PARylation and Counteracts PARP Inhibitor-Mediated Synthetic Lethality. *Cancer Cell* 33(6):1078-1093.e12. doi:



- 10.1016/j.ccell.2018.05.008. Erratum in: *Cancer Cell*. 2019 Jun 10;35(6):950-952. doi: 10.1016/j.ccell.2019.05.012.
14. James DI, Smith KM, Jordan AM, Fairweather EE, Griffiths LA, Hamilton NS, et al (2016) First-in-Class Chemical Probes against Poly(ADP-ribose) Glycohydrolase (PARG) Inhibit DNA Repair with Differential Pharmacology to Olaparib. *ACS Chem Biol* 11(11):3179-90. doi: 10.1021/acscchembio.6b00609.
  15. Essawy MM, El-Sheikh SM, Raslan HS, Ramadan HS, Kang B, Talaat IM et al (2021) Function of gold nanoparticles in oral cancer beyond drug delivery: Implications in cell apoptosis. *Oral Dis* 27:251-65 doi: 10.1111/odi.13551.
  16. Pijuan J, Barceló C, Moreno DF, Maiques O, Sisó P, Marti RM, et al (2019) In vitro Cell Migration, Invasion, and Adhesion Assays: From Cell Imaging to Data Analysis. *Front Cell Dev Biol* 7:107. doi: 10.3389/fcell.2019.00107.
  17. Franken NA, Rodermond HM, Stap J, Haveman J, van Bree C (2006) Clonogenic assay of cells in vitro. *Nat Protoc* 1(5):2315-9. doi: 10.1038/nprot.2006.339.
  18. Burry RW (2010) Immunocytochemistry: A Practical Guide for Biomedical Research. *Immunocytochemistry: A Practical Guide for Biomedical Research* (Springer New York, 2010). doi:10.1007/978-1-4419-1304-3.
  19. Liu YP, Zheng CC, Huang YN, He ML, Xu WW, Li B (2020) Molecular mechanisms of chemo- and radiotherapy resistance and the potential implications for cancer treatment. *MedComm* 2(3):315-40. doi: 10.1002/mco2.55.
  20. Geng L, Sun Y, Zhu M, An H, Li Y, Lao Y, et al (2023) The inhibition of PARG attenuates DNA repair in hepatocellular carcinoma. *Mol Biomed* 4(1):3. doi: 10.1186/s43556-023-00114-6.
  21. Sun Y, Zhang T, Wang B, Li H, Li P (2012) Tannic acid, an inhibitor of poly(ADP-ribose) glycohydrolase, sensitizes ovarian carcinoma cells to cisplatin. *Anticancer Drugs* 23(9):979-90. doi: 10.1097/CAD.0b013e328356359f.
  22. Shirai H, Poetsch AR, Gunji A, Maeda D, Fujimori H, Fujihara H, et al (2013) PARG dysfunction enhances DNA double strand break formation in S-phase after alkylation DNA damage and augments different cell death pathways. *Cell Death Dis* 4(6):e656. doi: 10.1038/cddis.2013.133.
  23. Bürkle A, Virág L (2013) Poly (ADP-ribose): PARadigms and PARadoxes. *Mol Aspects Med* 34(6):1046–65. doi: 10.1016/j.mam.2012.12.010.
  24. Sasaki Y, Nakatsuka R, Inouchi T, Masutani M, Nozaki T (2022). Inhibition of Poly (ADP-Ribose) Glycohydrolase Accelerates Osteoblast Differentiation in Preosteoblastic MC3T3-E1 Cells. *Int J Mol Sci*. 23(9):5041. doi: 10.3390/ijms23095041.
  25. Yu M, Chen Z, Zhou Q, Zhang B, Huang J, Jin L, et al (2022) PARG inhibition limits HCC progression and potentiates the efficacy of immune checkpoint therapy. *J Hepatol* 77(1):140-151. doi: 10.1016/j.jhep.2022.01.026.
  26. Matanes E, López-Ozuna VM, Oceau D, Baloch T, Racovitan F, Dhillon AK, et al (2021) Inhibition of Poly ADP-Ribose Glycohydrolase Sensitizes Ovarian Cancer Cells to Poly ADP-Ribose Polymerase Inhibitors and Platinum Agents. *Front Oncol* 11:745981. doi: 10.3389/fonc.2021.745981.
  27. Fauzee NJ, Pan J, Wang YL (2010) PARP and PARG inhibitors-new therapeutic targets in cancer treatment. *Pathol Oncol Res* 16(4):469-78. doi: 10.1007/s12253-010-9266-6.
  28. Cohausz O, Blenn C, Malanga M, Althaus FR (2008) The roles of poly(ADP-ribose)-metabolizing enzymes in alkylation-induced cell death. *Cell Mol Life Sci* 65(4):644-55. doi: 10.1007/s00018-008-7516-5.
  29. Houl JH, Ye Z, Brosey CA, Balapiti-Modarage LPF, Namjoshi S, Bacolla A, et al (2019) Selective small molecule PARG inhibitor causes replication fork stalling and cancer cell death. *Nat Commun* 10:5654 doi: 10.1038/s41467-019-13508-4.
  30. Li J, M Saville K, Ibrahim M, Zeng X, McClellan S, Angajala A, et al (2021) NAD<sup>+</sup> bioavailability mediates PARG inhibition-induced replication arrest, intra S-phase checkpoint and apoptosis in glioma stem cells. *NAR Cancer* 3(4):zcab044. doi: 10.1093/narcan/zcab044.
  31. Wang J, McGrail DJ, Bhupal PK, Zhang W, Lin KY, Ku YH (2020) Nucleostemin Modulates Outcomes of Hepatocellular Carcinoma via a Tumor Adaptive Mechanism to Genomic Stress. *Mol Cancer Res* 18(5):723-34. doi: 10.1158/1541-7786.MCR-19-0777.

### Citation

El Feky, S. E., Bekheet, N., Ibrahim, F., Abd El Moneim, N., Salama, M., Essawy, M., Haroun, M. PARG Inhibition Modulates Viability, Clonogenicity and Migration of Breast Cancer Cells Response to Radiotherapy. *Zagazig University Medical Journal*, 2024; (311-319): -. doi: 10.21608/zumj.2024.337569.3692